

THE EARLY SPECTRAL PHASE OF TYPE Ib SUPERNOVAE: EVIDENCE FOR HELIUM

R. P. HARKNESS AND J. C. WHEELER

Department of Astronomy and McDonald Observatory, University of Texas at Austin

B. MARGON¹

Department of Astronomy, University of Washington

R. A. DOWNES

Applied Research Corporation

R. P. KIRSHNER

Department of Astronomy, Harvard University

A. UOMOTO

Department of Physics and Astronomy, Louisiana State University

E. S. BARKER, A. L. COCHRAN, H. L. DINERSTEIN, AND D. R. GARNETT

Department of Astronomy and McDonald Observatory, University of Texas at Austin

AND

R. M. LEVREAUULT

Harvard-Smithsonian Center for Astrophysics

Received 1986 September 17; accepted 1986 November 11

ABSTRACT

Spectra covering the wavelength range 3500–7300 Å during the first 2 months of observation of the Type Ib supernovae (SN Ib) 1983N in NGC 5236 (M83) and 1984L in NGC 991 are compared with theoretical supernova atmosphere calculations based on power-law density structure ($\rho \propto r^{-n}$, $n \sim 7$). Evidence is presented for lines of He I at 4471, 4921, 5015, 5876, 6678, 7065 Å (and perhaps 7281 Å) and hence for substantial amounts of helium, the first confirmed evidence for helium in supernova ejecta near maximum light. The helium-level populations appear to depart strongly from LTE (departure coefficient $\gtrsim 10^2$).

The blue portion of the spectrum is dominated by blends of Fe II with the iron in approximately solar proportions by mass. At the same density and temperature, an iron mass fraction as large as 0.1 gives features which are far too strong throughout the spectrum, implying that SN Ib do not arise in detonating white dwarfs. The prominent absorption feature at 6300 Å is plausibly C II $\lambda 6580$, although a non-LTE contribution from Ne I $\lambda 6402$ cannot be ruled out. Emission features of [O I] at 5577 and 6300 Å are observed after about 20 days, presaging the transition to the oxygen-dominated “supernebular” phase observed 8–14 months after maximum in SN 1983N, 1984L, and 1985F.

The power-law models for the ejecta structure are consistent with a relatively large mass ($\gtrsim 5 M_{\odot}$) and kinetic energy ($\gtrsim 5 \times 10^{51}$), but rigorous lower limits have not been established. The theoretical spectra do not constrain the maximum amount of mass but, for the current models, $M \gtrsim 10 M_{\odot}$ implies uncomfortably large kinetic energies, $\gtrsim 10^{52}$ ergs.

The conclusions concerning substantial mass and a large helium abundance with solar proportions of iron add to the evidence that SN Ib have their origin in the cores of relatively massive stars. If so, SN Ib represent the first opportunity to study directly the structure and composition of the final stage of evolution of massive stars and to explore the mechanism of their explosion.

Subject headings: stars: abundances — stars: supernovae

I. INTRODUCTION

Recent observations of supernovae SN 1983N and SN 1984L have focused attention on the class of “peculiar” Type I supernovae (Wheeler and Levreault 1985; Elias *et al.* 1985; Panagia *et al.* 1987; Uomoto and Kirshner 1985; Branch 1986). They have been designated SN Ib to formally distinguish them from classical Type I events, SN Ia. The SN Ib are apparently hydrogen deficient at maximum light. They do not display the absorption feature at 6150 Å identified with Doppler-shifted Si II $\lambda 6355$ which characterizes SN Ia, but SN 1983N and 1984L do have an absorption at 5700 Å and other

distinguishing spectral features. They are dimmer than SN Ia by about 1.5 mag, and hence comparable to Type II (plateau) events. The shape of the optical light curve of SN 1983N is similar to that of SN Ia near peak light, with the rise perhaps somewhat slower (Panagia *et al.* 1987). SN 1983N is slightly off-center from a large H II region complex in M83 (Richter and Rosa 1983). A careful determination of the location of the supernova on a Palomar Observatory Sky Survey print shows that SN 1984L is coincident with an H II region in NGC 991, as suggested by Wheeler and Levreault (1985). Infrared light curves seem to distinguish between SN Ia and SN Ib (Elias *et al.* 1985). Detection of the 1.644 μm line of [Fe II] 360 days after optical maximum in SN 1983N suggests the presence of $\sim 0.3 M_{\odot}$ of iron in the ejecta (Graham *et al.* 1986). SN 1983N

¹ Visiting Astronomer, Kitt Peak National Observatory, which is operated by AURA, Inc., under contract to the National Science Foundation.

and SN 1983L have been detected in the radio (Sramek, Panagia, and Weiler 1984; Panagia, Sramek, and Weiler 1986), indicating the presence of a circumstellar nebula, presumably produced by a wind (Chevalier 1984).

Spectra of SN 1983N obtained 8 months after maximum light (Gaskell *et al.* 1986) and of SN 1984L 14 months after maximum (Kirshner 1986) are very different than spectra near maximum light. The later spectra display strong broad lines of [O I] $\lambda\lambda$ 6300, 6364, Mg I] λ 4571, Na I D $\lambda\lambda$ 5890, 5896, and [Ca II] $\lambda\lambda$ 7291, 7324. SN 1985F (Filippenko and Sargent 1985, 1986) showed similar features and is projected onto and presumably spatially near an H II region. Although only discovered of order 8 months after maximum, SN 1985F must be of a similar nature to SN 1983N and SN1984L, namely an SN Ib in the "supernebular" phase (cf. Wheeler *et al.* 1986; Gaskell *et al.* 1986).

In § II we present a near-infrared spectrum and several optical spectra of SN 1983N obtained over a period from 10 days before maximum light to about a week after maximum (see also Panagia *et al.* 1987) and of SN 1984L from about maximum light to about 60 days later. On the basis of these spectra we argue for the first definite identification of helium in supernova ejecta near maximum light. We also identify the emergence of oxygen emission lines which presage the dramatic transition to the supernebular phase. In §§ III and IV we present supernova atmosphere models which are consistent with the observations and argue that a strong departure of helium level populations from LTE is necessary. In § V we summarize the current status of SN Ib, the arguments that they result from core collapse in moderately massive stars, and some of the immediate work necessary to further clarify the nature of these events.

II. OBSERVATIONS

The observations of SN 1983N were all made on the 1.3 m telescope of the McGraw-Hill Observatory. The spectra of July 19 and July 27 are also presented by Panagia *et al.* (1987). Observations of SN 1984L were made by Barker, Cochran, Dinerstein, Garnett, and Levreault at McDonald Observatory and by Margon and Downes at KPNO, Mount Lemmon, and Lick Observatory. A journal of observations is given in Table 1.

TABLE 1

JOURNAL OF OBSERVATIONS

Supernova	Date	Observer	Telescope	Device	Resolution (Å-FWHM)
SN 1983N.....	1983 Jul 7	Uomoto	McGraw-Hill 1.3 m	Mark III grism spectrometer	10
	1983 Jul 17	Moody	McGraw-Hill 1.3 m	Mark II intensified reticon scanner	12
	1983 Jul 18	Moody	McGraw-Hill 1.3 m	Mark II intensified reticon scanner	12
	1983 Jul 19	Moody	McGraw-Hill 1.3 m	Mark II intensified reticon scanner	12
	1983 Jul 27	Johns	McGraw-Hill 1.3 m	Mark II intensified reticon scanner	12
SN 1984L	1984 Aug 30	Levreault	McDonald 2.7 m	Intensified dissector scanner	10
	1984 Aug 31	Levreault	McDonald 2.7 m	Intensified dissector scanner	10
	1984 Sep 3	Margon	KPNO 2.1 m	Intensified image dissector scanner	13
	1984 Sep 4	Margon	KPNO 2.1 m	Intensified image dissector scanner	13
	1984 Sep 19	Barker/Cochran	McDonald 2.7 m	Intensified dissector scanner	10
	1984 Sep 23	Downes	Mount Lemmon 1.5 m	Image tube scanner	13
	1984 Sep 28	Downes	Mount Lemmon 1.5 m	Image tube scanner	13
	1984 Sep 29	Downes	Mount Lemmon 1.5 m	Image tube scanner	13
	1984 Sep 30	Downes	Mount Lemmon 1.5 m	Image tube scanner	13
	1984 Oct 18	Dinerstein/Garnett	McDonald 2.7 m	Intensified dissector scanner	10
	1984 Oct 31	Downes	Lick 3 m	Image tube scanner	13
1984 Nov 1	Barker/Cochran	McDonald 2.7 m	Intensified dissector scanner	10	

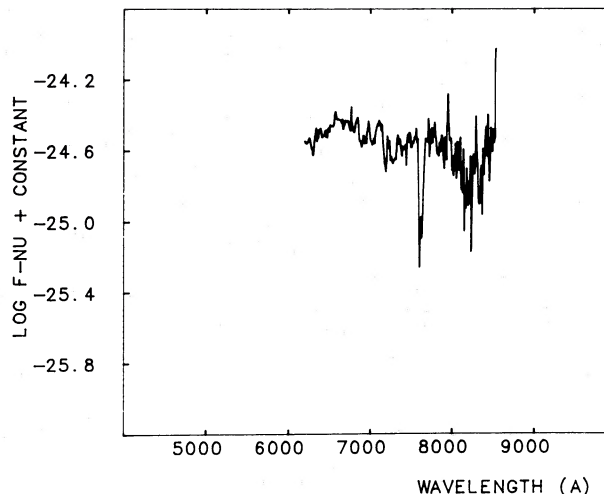


FIG. 1.—The logarithm of the flux distribution F_ν as a function of wavelength (Å) for the Type Ib supernova 1983N in NGC 5236 (M83) is presented for 1983 July 7, about 10 days prior to maximum. A redshift correction of 275 km s⁻¹ has been applied. Note the broad absorption feature at about 8200 Å which is attributable to the Ca II infrared triplet.

Figure 1 gives a near-infrared spectrum of SN 1983N obtained at McGraw-Hill Observatory by A. Uomoto on July 7, about 10 days before maximum. A 2"5 slit was used. Conditions were not photometric. Figure 2 presents a time series of spectra obtained at McGraw-Hill Observatory by M. Johns and J. W. Moody of SN 1983N spanning 10 days. The spectrum from July 17 was obtained at very nearly the phase of maximum light detected by the Fine Error Sensor (FES) on the *IUE* satellite, the response of which corresponds approximately to *V* magnitude (Panagia *et al.* 1987). Since SN 1983N was observed at high airmass (declination $\sim -29^\circ$), the problem of properly correcting for atmospheric extinction and differential refraction may be significant. There is a suggestion in Figure 2 of a gradual reddening of the spectrum over the 3 days near maximum light which seems to be a definite effect by the epoch of the July 27 spectrum. This is qualitatively consistent with the photometric behavior of SN 1983N and of SN 1962L, another SN Ib candidate, but quantitatively too steep.

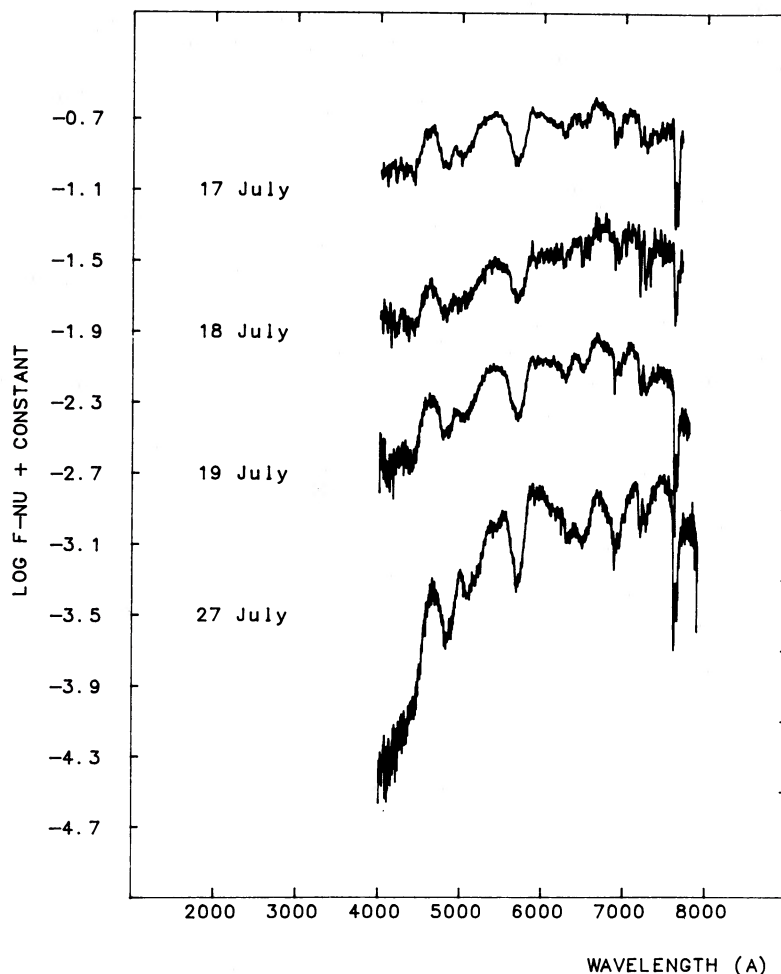


FIG. 2.—The logarithm of the flux distribution F_ν as a function of wavelength (\AA) for SN 1983N is given from near maximum light (peak $V \sim 1983$ July 17; Panagia *et al.* 1987) to about 10 days after maximum. A redshift correction of 275 km s^{-1} has been applied, but no reddening correction. Spacings between individual spectra are arbitrarily chosen for clarity. Narrow absorption features between 6830 and 7625 \AA are due to Earth's atmosphere. Note the absence of conspicuous H α and of the 6150 \AA absorption that typifies Type Ia supernovae.

The spectra in Figure 2 can be integrated over appropriate filter responses (Allen 1973, pp. 197, 201) to give $B - V = 0.60, 0.67, 0.97,$ and 1.94 for the spectra of July 17, 18, 19, and 27, respectively. The first two points fall along the $B - V$ color curve for SN 1983N determined by photometric measurements about 5 days prior to and about 5–15 days after optical maximum (Panagia *et al.* 1987). The third point is too red, suggesting that the slope of the July 19 spectrum is not trustworthy. The color of the July 27 spectrum ($B - V = 1.94$) is in direct conflict with photometric observations at about the same epoch ($B - V \sim 1.1$; Panagia *et al.*). The color curve of SN 1983N is roughly parallel to that of SN 1962L (Bertola 1964), but bluer by about 0.2 mag. It is about 0.7 mag redder than the standard curve defined by SN Ia (Pskovskii 1970).

Figure 3 shows a time series of spectra of SN 1984L. The first is that previously published by Wheeler and Levreault (1985), and the remaining were obtained by Levreault, Margon, Downes, Barker, Cochran, Dinerstein, and Garnett. These spectra also show a gradual tendency to redden, although the slope does not change appreciably from August 30 to September 3. There is an appreciable change in slope by September 19. Table 2 gives photometric magnitudes derived from the spectra of Figure 3. The resulting V and B light curves are somewhat

flatter than those of SN 1962L and SN 1983N. With the exception of the August 31 spectrum, the color is very close to that of SN 1983N near maximum, and to the single photoelectric point, $B - V = +0.49$ (Buta 1984). For epochs 20–60 days past

TABLE 2
PHOTOMETRIC COLORS DERIVED FROM SPECTRA OF SN
1984L

Date (1983)	B	V	$B - V$
Aug 30	14.64	14.10	0.45
Aug 31	15.61	14.71	0.90
Sep 3	14.66	14.08	0.58
Sep 4	14.71	14.75 ^a	...
Sep 19	15.51	14.45	1.06
Sep 23	15.84	14.58	1.26
Sep 28	15.67	14.57	1.07
Sep 29	16.15	14.95	1.20
Sep 30	16.23	14.97	1.26
Oct 18	16.64	15.50	1.14
Oct 31	16.92	15.59	1.33
Nov 1	16.29	15.12	1.17

^a Lower limit to flux in V band. Spectrum does not extend to red limit.

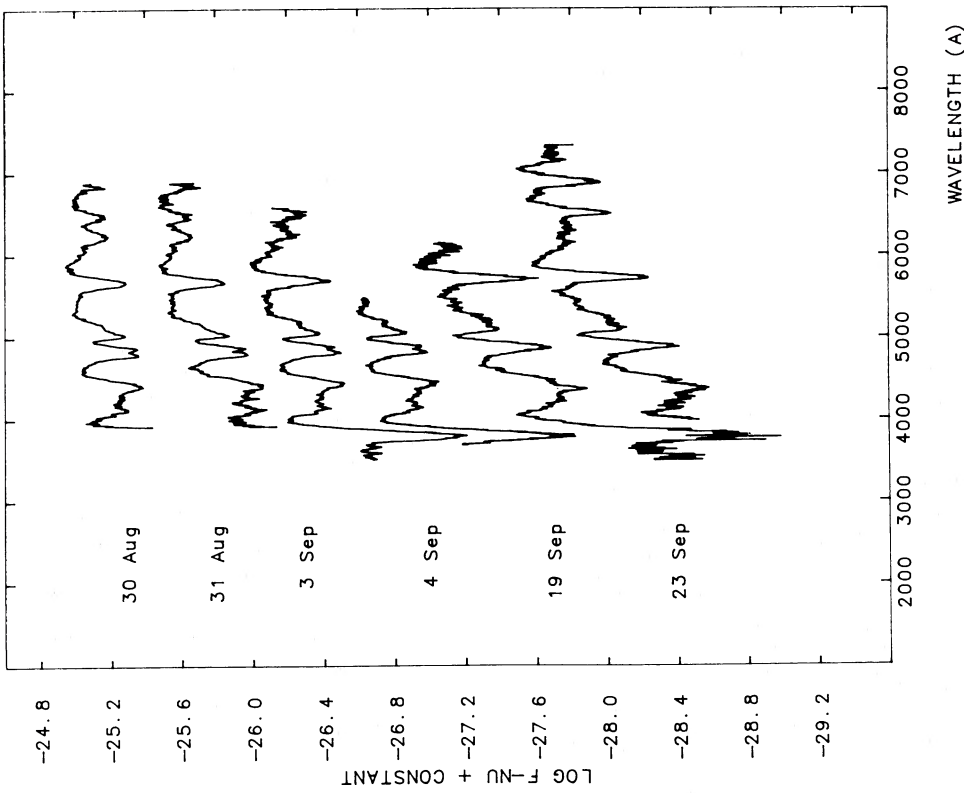


FIG. 3a

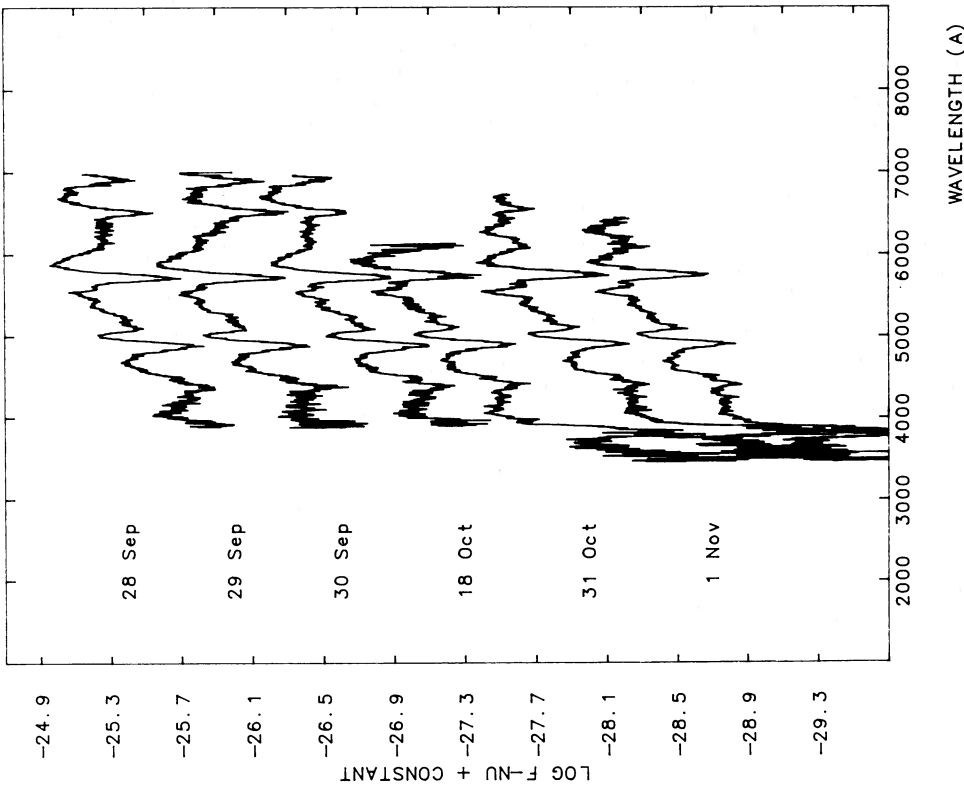


FIG. 3b

FIG. 3.—(a) The logarithm of the flux distribution F_{ν} as a function of wavelength (\AA) for the Type Ib supernova 1984L in NGC 991 is given from near maximum light (see text, Table 2) to about 20 days after maximum. A redshift correction of 1606 km s^{-1} has been applied, but no reddening correction. The first spectrum is presented at the observed flux level ($\text{ergs s}^{-1} \text{Hz}^{-1}$), but all others are spaced for clarity. Narrow absorption features between 6830 \AA and 7625 \AA are due to Earth's atmosphere. Note the basic similarity to the spectra of Fig. 2 (b) but for spectra from about 30 to about 60 days after maximum light.

V maximum the color from Table 2 is nearly constant at $B-V \sim 1.2$. In contrast, SN Ia reach such values at their reddest but show a blueward trend in $B-V$ beginning ~ 30 days past maximum (Pskovskii 1970).

Although the time of maximum light is not known precisely, it is thought to have been around September 1 (the two spectra from August 30 and September 3 have the same flux at 5500 Å; see also Table 2). A remarkable feature of the spectra of Figure 3 is then their striking homogeneity. The evolution of the spectrum is much less distinct than that displayed for SN Ia (Branch *et al.* 1983). Between September 3 and September 23, the absorption feature at 6300 Å has disappeared, but all the other major features are reproduced. During a similar 2 week period after maximum light, SN 1981B underwent significant spectral changes, although the subsequent evolution in the spectrum was quite small. There is an odd change in slope in the September 29 spectrum as compared to September 28 and 30 between 6150 Å and 6500 Å. There is no obvious systematic problem that could affect only the few hundred channels covering this wavelength range, and otherwise the spectral agreement is excellent. This behavior is currently unexplained.

The large oxygen abundance manifested in the supernebular phase of SN Ib (Gaskell *et al.* 1986) suggests that there might be evidence for oxygen at earlier times as well. A study of Figures 2 and 3 shows that this is so. Evidence for broad emission of [O I] $\lambda 5577$ begins to be apparent in the July 27 spectrum of SN 1983N and the September 19 spectra of SN 1984L. This line is very prominent in the October 31 and November 1 spectra of SN 1984L which also give the first evidence for [O I] $\lambda 6300$ which emerges as the dominant supernebular line in SN 1983N, SN 1984L, and SN 1985F.

Figure 4 shows a comparison of spectra of the Type Ia event SN 1981B with those of SN 1983N and SN 1984L at roughly comparable epochs, near maximum light and 10–20 days later. Although there is some similarity between SN 1981B March 6–9 and SN 1983N July 19 and SN 1984L August 30 in the wavelength range 3500–4600 Å (note SN 1984L does show the distinct absorption at 3800 Å in the September 3 spectrum which is presumed to be Ca II H and K), there are major differences throughout the longer wavelength range. In contrast, while there are some differences in detail between the spectra, more so than between two SN Ia at similar epochs, the

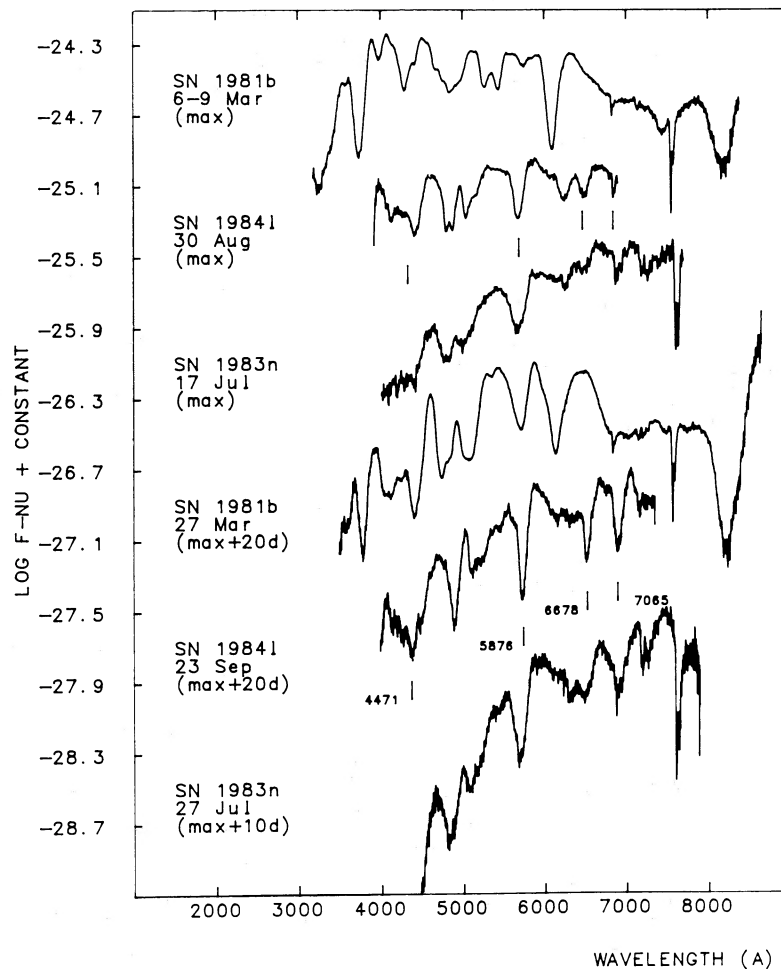


FIG. 4.—Spectra of the Type Ia supernova 1981B in NGC 4536 near maximum light and about 20 days later are compared with spectra of the Type Ib supernovae 1983N and 1984L near maximum light and about 10 and 20 days after maximum, respectively. All spectra are presented in the rest frame of the host galaxy. Note the 6150 Å absorption in the SN Ia which is absent in the SN Ib and the strong absorption at 5700 Å in the SN Ib which has no counterpart in the SN Ia.

close resemblance of the spectra of SN 1983N and SN 1984L near maximum and again 10–20 days later establishes that they are of the same class of explosive event.

A comparison of the *maximum* light spectra of the two SN Ib events with the 3 week postmaximum spectrum of SN 1981B on March 27 shows a much closer resemblance at all wavelengths less than 6000 Å. The spectra are still quite different at wavelengths greater than 6000 Å. This agreement in the blue has given rise to the aphorism that SN Ib are “born old” or are “precocious” since early on they resemble more mature SN Ia. The agreement between the blue range of postmaximum SN Ia and SN Ib is not quite as good for the September 23 spectrum (and later) of SN 1984L. The peak at 4000 Å near maximum light for the SN Ib events finds a match at slightly shorter wavelength in the March 27 spectrum of SN 1981B (Branch *et al.* 1983). This feature disappears in the later SN Ib spectra (cf. Fig. 2) whereas it remains prominent in the evolving spectra of SN 1981B. The sharp peak at 5000 Å in SN 1984L seems to correspond to a feature in the March 27 spectrum of SN 1981B, but the feature in SN 1984L starts to the red of that in SN 1981B and evolves a little farther to the red, whereas the feature in SN 1981B is rather static with time (Branch *et al.* 1983). Again the later time spectra of the SN Ia and b are quite different at wavelengths in excess of 6000 Å.

The fiducial marks shown in Figure 4 represent wavelengths of the strongest expected lines of He I, blueshifted by 10,000 km s⁻¹ for the early spectra and 7500 km s⁻¹ for the later ones. The striking agreement with observed minima corresponding to the rest wavelength of He I lines at 4471, 5876, 6678, and 7065 Å, particularly in the later spectra, is convincing evidence that He is a significant constituent of the ejecta of SN Ib as observed at this phase, the first 2 months. There is a hint of the He I 7281 Å line in the September 23 spectrum of SN 1984L, but this line may not contribute as strongly. There appears to be a peak at the expected absorption minimum of 7281 Å for the spectra of SN 1983N. The He I 4921 and 5015 Å lines and Fe II 4923 and 5018 Å lines probably contribute to the absorption feature at 4900 Å, as we demonstrate in the next section. The absorption at 6300 Å in the maximum light spectra must have some origin other than He I, since there are no candidate He I lines.

III. PHYSICAL MODELS

As a first attempt at modeling SN Ib spectra, power-law density and temperature profiles with homogeneous composition have been assumed. The velocity profile will be homologous to high accuracy at the phases of interest. The inner radius of the supernova “atmosphere” was chosen to correspond to the propagation of ejected mass for 20 days at 5000 km s⁻¹, giving $r_{\text{inner}} = 8.6 \times 10^{14}$ cm. The temperature was chosen to be $T_{\text{inner}} = 11,700$ K and to decrease in the atmosphere according to $T \propto r^{-1/2}$. This fixed temperature distribution was used to isolate the effects of variation in

composition and ad hoc deviations from Boltzmann excitation equilibrium. The density was assumed to vary as $\rho \propto r^{-n}$, with $n = 5, 7, 10$. The total mass included in the atmosphere is formally $31 M_{\odot}$. Most of this mass is at large optical depth and does not contribute significantly to the formation of the spectrum (see below). At constant total mass, the density at the inner boundary varies with the slope of the density distribution. The outer radius was chosen to correspond to a density 10^5 times less than that at the inner boundary. The outer temperature varies accordingly. Relevant parameters for the three density distributions are given in Table 3. These parameters give typical “photospheric” values for velocity (~ 7500 km s⁻¹) and temperature (~ 9000 K). The kinetic energies in Table 3 are formal values for the adopted mass, not to be taken literally. The kinetic energy provides a constraint on the mass of the ejecta for given velocity structure (see below).

Observations imply that a large oxygen abundance is necessary to explain the late-time spectra of SN Ib (Gaskell *et al.* 1986). The previous section gives preliminary evidence that a considerable mass of helium is visible near maximum light and for at least 2 months afterward. Evolutionary calculations for massive stars give C/O ratios < 1 by mass (cf. Prantzos *et al.* 1986). On this basis, two homogeneous composition models have been considered: (1) approximately 0.9 He, 0.01 C, and 0.09 O by mass (“helium” models), and (2) approximately 0.1 He, 0.1 C, and 0.8 O by mass (“oxygen” models). In both cases heavier elements are present in the same proportion by mass as they are in the Sun. Emergent fluxes were obtained using the supernova atmosphere code described by Harkness (1985, 1986, 1987). The resulting spectra are presented for structures with $\rho \propto r^{-7}$ in Figures 5 and 6 for the helium-rich and oxygen-rich models, respectively. The luminosity varies with the opacity and hence the composition, but for both sets of models is $\sim 2.5 \times 10^{42}$ ergs s⁻¹.

The properties of these SN Ib model atmospheres differ in several ways when compared to those for SN Ia. SN Ia models with iron-rich cores and O/Si envelopes are nearly optically thin near maximum light because the optical continuum opacity is due almost entirely to electron scattering. The ratio of absorption to scattering is typically 1/50 at optical frequencies; hence the true photosphere is not coincident with the surface of last scattering and a range of temperature and density conditions are reflected in the overall emergent flux. The opacity of the iron-rich core is lower than that of the mixture of intermediate mass elements in the envelope. When the latter becomes optically thin, there is a rapid transition to the iron-dominated phase, occurring less than 2 weeks after maximum light. Conditions in SN Ib are generally similar except that a much greater mass is involved. On the basis of the late-time observations, one expects a core consisting predominantly of oxygen and other intermediate mass elements. The envelope is presumed to contain a large mass fraction of helium, which contributes negligible continuous absorption at

TABLE 3
PARAMETERS FOR $31 M_{\odot}$ POWER-LAW ATMOSPHERE: $\rho \propto r^{-n}$

n	R_{in} (cm)	R_{out} (cm)	v_{in} (km/s)	v_{out} (km/s)	T_{in} (K)	T_{out} (K)	ρ_{in} (g/cm ³)	ρ_{out} (g/cm ³)	K.E. (ergs)
5.....	8.6×10^{14}	8.6×10^{15}	5000	50000	11700	3700	1.5×10^{-11}	1.5×10^{-16}	1.3×10^{52}
7.....	8.6×10^{14}	4.5×10^{15}	5000	26200	11700	5145	3.1×10^{-11}	3.1×10^{-16}	1.5×10^{52}
10.....	8.6×10^{14}	2.7×10^{15}	5000	15700	11700	6600	5.4×10^{-11}	5.4×10^{-16}	1.5×10^{52}

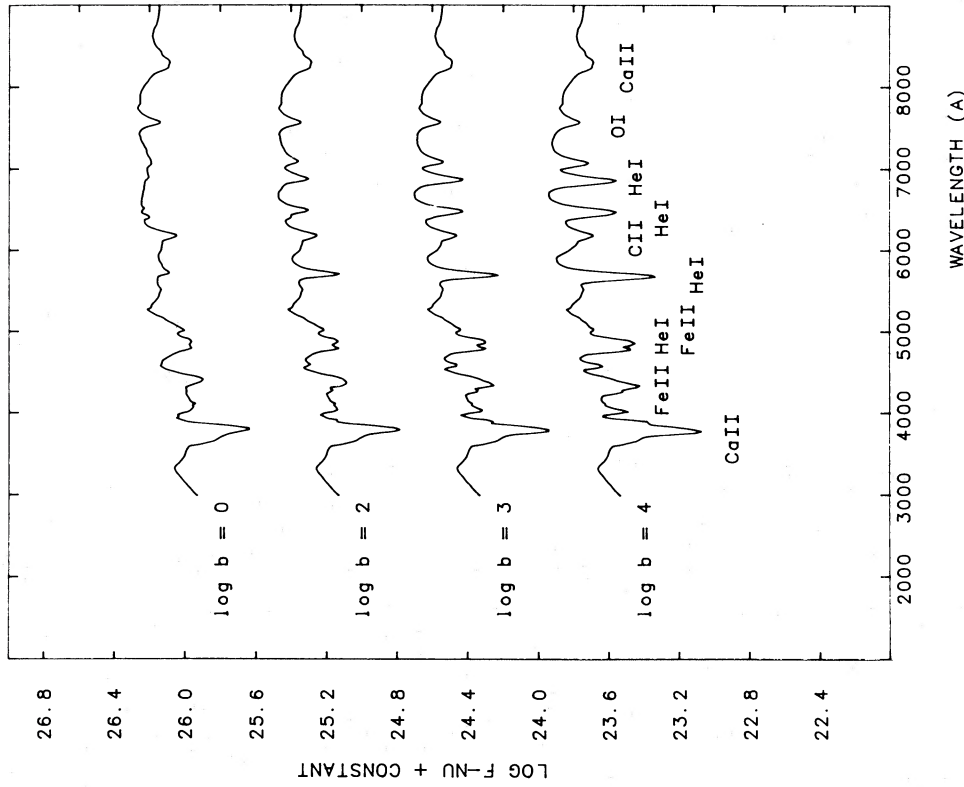


FIG. 5

FIG. 5.—A series of theoretical spectra are presented for a model with a power-law density profile, $\rho = 3.1 \times 10^{-11} \text{ g cm}^{-3} (r/r_0)^{-7}$ for $r > r_0 = 8.6 \times 10^{14} \text{ cm}$. The velocity and temperature vary as $v = 5000 \text{ km s}^{-1} (r/r_0)$ and $T = 11,700 \text{ K} (r/r_0)^{-1/2}$, respectively. The total mass is formally $31 M_\odot$, of which only the outer $9 M_\odot$ substantially affects the spectrum. The composition is approximately $X_{\text{He}} = 0.9$, $X_{\text{C}} = 0.01$, $X_{\text{O}} = 0.09$ with heavier elements in solar ratios. Spectra are labeled by the logarithm of the departure coefficient, b , by which the Boltzmann level populations of helium have been multiplied. A reddening corresponding to $A_V = 0.5$ has been assumed. Note the weakness of the helium lines for $b = 1(\text{L,TE})$ and the growing strength of the helium features for $b > 1$.

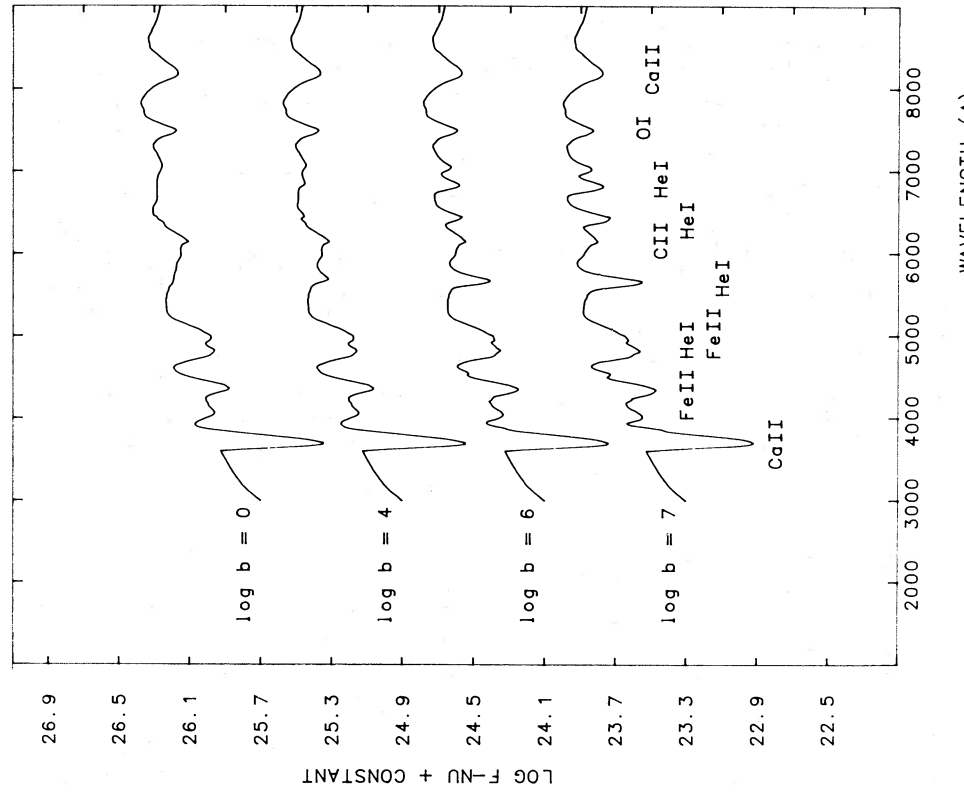


FIG. 6

FIG. 6.—Same as Fig. 5, but for a composition of approximately $X_{\text{He}} = 0.1$, $X_{\text{C}} = 0.1$, and $X_{\text{O}} = 0.8$. Of the $31 M_\odot$ in the model, only the outer $4.5 M_\odot$ substantially affect the spectrum. Note that with a larger contribution to electron scattering opacity associated with the increased oxygen abundance, a larger departure coefficient is required to reproduce He I lines of a given strength compared with Fig. 5.

low temperatures. Any assumed departure from LTE, however, also enhances the bound-free opacity due to He I. When the departure from LTE is large, as for some of the models presented below, the absorptive opacity may rival electron scattering, giving rise to an emergent spectrum more characteristic of local conditions near the photosphere.

At the temperatures and densities typical of supernovae near maximum light, it proves to be exceptionally difficult to excite any of the visible lines of helium. In LTE atmospheres for main-sequence stars, He I lines are only visible in B stars where the helium is already appreciably ionized. With supernova ambient conditions there is never sufficient contrast for the lines to be visible if a significant fraction of the helium is ionized due to the relatively large electron density per gram available from a nearly pure helium atmosphere (compared to, say, a predominantly O/Si atmosphere in SN Ia). The LTE calculations shown as the top trace in Figures 5 and 6 display almost no evidence of the helium lines which become so prominent in SN Ib. The helium lines can be made apparent, however, by scaling the Boltzmann level populations by some departure coefficient, b . In these exploratory calculations, b is taken to be the same for all levels and independent of radius. Figures 5 and 6 also present theoretical spectra with departure coefficients $b = 10^2, 10^3, \text{ and } 10^4$ for the "helium" models and $b = 10^4, 10^6, \text{ and } 10^7$ for the "oxygen" models. For the "helium" atmosphere a factor of 100 suffices to match the observed line strengths. For the "oxygen" atmosphere a much larger value is required, again due to the need to have a large contrast of line over electron scattering opacity. The electron scattering opacity is considerably enhanced in the oxygen atmosphere relative to the helium atmosphere for the same temperature and density and so, for a given mass, the oxygen atmosphere has a far greater electron scattering optical depth. Since lines are diluted by larger electron scattering opacity, the features due to C II $\lambda 6580$ and O I $\lambda 7773$ are not significantly stronger in the spectra with larger oxygen and carbon abundances. Although the "helium" and "oxygen" atmospheres and resulting spectra are similar for appropriate choices of b , the features fall more to the blue in the latter case. This is again a result of the larger electron scattering optical depth so that lines tend to form farther out in higher velocity material.

Although the requisite departure coefficient to match the observed spectra decreases as the He/O ratio is increased, suggesting some preference for a larger helium abundance, a pure helium composition can be ruled out for the current models. The ionization structure depends on the free electron density, and hence the composition, for a given density and temperature structure. For the conditions assumed, a pure helium atmosphere would be essentially neutral and optically thin to electron scattering. The resulting spectrum would bear no relation to the observations. Some element of significantly lower ionization potential than helium, e.g., carbon or oxygen, must exist in moderate abundance to provide the requisite supply of free electrons.

Atmosphere calculations for different density profiles, $\rho \propto r^{-5}, r^{-10}$, gave much less satisfactory results. The shallower density profile puts more mass at large radii where the temperature ($\propto r^{-1/2}$) is low. This results in strong lines of Fe II and other species being formed at high velocity, with a larger radiating surface. The resulting spectral features are far too broad. The steeper profile produces an atmosphere which is more compact. The bulk of the matter is then at lower velocities, but the lines appear to be too narrow. A strong state-

ment as to whether a steeper density profile can be ruled out cannot be made at this time, due to the limitations of our power-law density model. One model was run with the $\rho \propto r^{-7}$ profile, but with the temperature reduced by a factor of $2^{1/2}$. The result was a satisfactory model in many respects, but it required $b = 10^{10}$ to reproduce the He I line strengths.

In Figures 5 and 6 the total mass is $31 M_{\odot}$, but this can be reduced to about 9 and $4.5 M_{\odot}$ for the helium and oxygen atmospheres, respectively, without altering the emergent flux significantly. We were unable to determine a lower mass limit due to complications in setting the inner boundary conditions when the total electron scattering optical depth becomes small. With the assumed velocity profile the nominal kinetic energy for the full $31 M_{\odot}$ is 1.5×10^{52} ergs, excessive by most estimates. The outer $9 M_{\odot}$ has 7.5×10^{51} ergs and the outer $4.5 M_{\odot}$, 5.2×10^{51} ergs. A challenge for more realistic models will be to determine appropriate density and composition structures which satisfy the observed spectra but do not require too large a kinetic energy.

At present, we have no physical mechanism to explain why the He I level populations should show such large departures from LTE. It is conceivable that He I lines of the observed strengths could be formed in a more complex LTE density/temperature structure than the one we have assumed. Höflich, Wehrse, and Shaviv (1986) have, however, shown that $b \sim 10\text{--}30$ can be obtained for the lower levels of hydrogen in the outer atmospheres of Type II supernovae. It is not unreasonable to assume that helium may show even larger deviations under similar conditions simply because of the much larger separation of the excited states from the ground state (~ 20 eV). Indeed, even in LTE the level populations are extremely sensitive to temperature for $T < 10,000$ K.

We have employed the same departure coefficient for all of the excited states of He I. Furthermore, this value is assumed to be independent of radius, although, in general, one would expect larger values at lower densities where collisions are less capable of ensuring LTE. The resulting relative line strengths for 5876, 6678, and 7065 Å are in fair accord with the corresponding features of the observed spectra. That this should be so is not obvious: one might expect significant differences between the singlets and triplets. Failure of the approximation of a constant departure coefficient may already be apparent in the models where both blue lines, especially 4471 Å and the red line at 7281 Å, appear to be too strong in the theoretical calculations. The 4471 Å line can be seen distinctly only in the September 19 and later spectra of SN 1984L, whereas it contributes significantly in all the model spectra which display 5876 Å at an appropriate strength. It is not clear whether any feature corresponding to the predicted 7281 Å line is present in either SN 1983N or SN 1984L.

It is important to stress the ad hoc nature of these models. Only the simplest attempt has been made to assure that they are self-consistent in the sense that the adopted structure (and opacity) corresponds to the phase of the observed spectra, e.g., maximum light or shortly thereafter. Furthermore, no consideration has been given to the heating mechanism responsible for maintaining the energy output.

IV. INTERPRETATION OF THE SPECTRA

Figure 7 shows the near-maximum light spectra of SN 1983N and SN 1984L together with a theoretical spectrum of the "helium" case with $b = 10^2$. The He I lines at 5876, 6678,

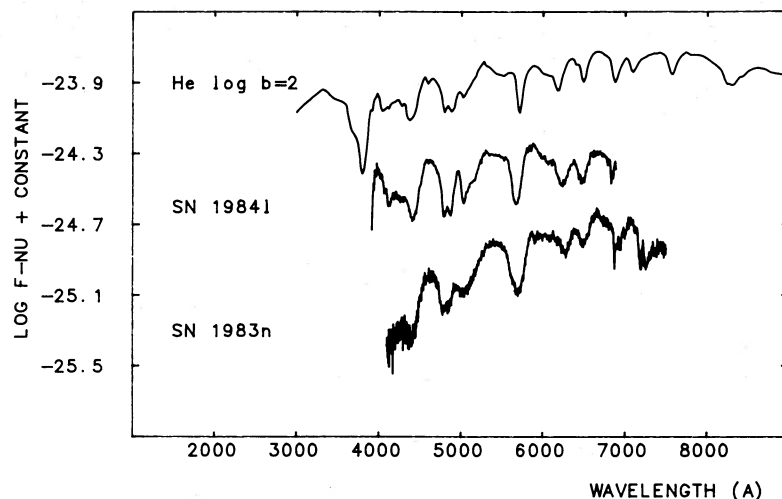


FIG. 7.—The spectra of SN 1983N and SN 1984L near maximum light are shown in comparison with the theoretical calculation of Fig. 5, with $b = 10^2$. The model provides generally good agreement with the strength and position of the features throughout the observed portion of the spectrum. In the model, the absorption feature at 6200 Å is C II λ 6580, suggesting that this line may contribute to the observed minimum at 6300 Å. O I and Ca II are predicted to have significant features in the near-IR.

and 7065 Å are easily identified. In the absence of a physical model for the structure of the atmosphere and lacking a definite mechanism for departures from LTE, we can only assert that moderately large departures from LTE (i.e., ~ 100 in the “helium” case) are more plausible than the extreme departures apparently necessary in atmospheres where helium is only a minor constituent. We therefore suggest that the He/O ratio is closer to 10 rather than, say, 0.1 in the outer layers of SN 1983N and 1984L.

Evidence for oxygen appears in the theoretical models only in the feature at ~ 7500 Å, which is due to O I 7773 Å. This feature is contaminated by terrestrial lines in SN 1983N (Figs. 1 and 2), and not obviously present although at the predicted strength and breadth some evidence might be expected anyway. It falls too far to the red to be seen in any of the spectra of SN 1984L (Fig. 3). Calcium H and K is apparent in some of the spectra of SN 1984L, while the Ca II 8466 triplet was observed in SN 1983N about 10 days prior to maximum (Fig. 1). Both observed features are somewhat stronger than the calcium lines in the theoretical models.

In the blue, the emergent spectrum is due mainly to blends of Fe II, Mg II with some contribution from neutral helium. Note that, unlike SN Ia which seem to require an appreciable enhancement of the iron-peak abundances in the matter visible near optical maximum (Branch *et al.* 1985; Wheeler and Harkness 1986; Wheeler *et al.* 1986), the spectra of SN Ib can be accounted for with essentially solar abundances of elements heavier than oxygen. This is apparently due to a combination of factors, including the lower velocity of expansion and the greater total mass.

There are some small but notable differences between the spectra of SN 1983N and SN 1984L. The width of the helium lines seems to indicate a somewhat higher expansion velocity in SN 1983N. Note in the theoretical spectra of Figure 5 the double notch at 4900 Å due to Doppler-shifted 4921 and 5015 Å lines of He I. This feature clearly shows in the August 30–September 4 spectra of SN 1984L. This feature is not apparent in the spectra of SN 1983N, and the minimum there is probably due to the 4923 and 5018 Å lines of Fe II as it is in the theoretical spectra of Figure 6, except at the largest departure coefficient ($b = 10^7$). An attempt has not yet been made to find

a combination of helium abundance and departure coefficient that reproduces the 5876 Å line without a noticeable contribution from the 4921 and 5015 Å lines.

One notable feature of SN Ib which remains in doubt is the line appearing at around 6300 Å. This line is discernible in the SN 1984L spectrum of August 30, much less so in the spectrum of 4 days later and not seen thereafter, while it is most apparent in the July 19 spectrum of SN 1983N. In all of the model spectra shown here the closest plausible feature is due to C II λ 6580 with negligible contributions from Fe II and Ne I. The feature in the models is sensitive to the velocity and density profile. The disappearance of this feature can be understood qualitatively as a decrease in the excitation of C II, but since substantial departures from LTE are required in order to explain the helium lines all of the above identifications remain in some doubt, e.g., Ne I λ 6402 could contribute if enhanced by non-LTE effects.

Figure 8 shows a comparison of the spectrum of SN 1984L on September 23 and a “helium” theoretical spectrum with $b = 10^4$ at effectively maximum light conditions of luminosity and temperature. This observation clinches the identification of helium in SN Ib since $\lambda\lambda$ 4471, 5876, 6678, and 7065 are manifestly present. Although the density in the theoretical model in Figure 8 has not been scaled down, it should be about a factor of 10 less at this epoch than at maximum light ($\rho \propto t^{-3}$). This may account for the apparent increase in the departure coefficient and the appearance of [O I] λ 5577. Presumably an even higher value of b might be necessary at this epoch because of the overall matter/radiation temperature has clearly declined from maximum light.

In more realistic models, one would expect that there will be significant stratification of elemental abundances, and the models described here have not addressed that aspect. A preliminary model in which the abundances were chosen to be the same as the “oxygen” case for $v < 7000$ km s $^{-1}$ and the same as the “helium” case for $v > 7000$ km s $^{-1}$ did not show any marked improvement over “helium” atmospheres, but the position (in velocity) of the interface may be important.

The model for SN Ib suggested by Branch and Nomoto (1986) is based on the detonation of a layer of degenerate helium surrounding a degenerate C/O core. After freezeout

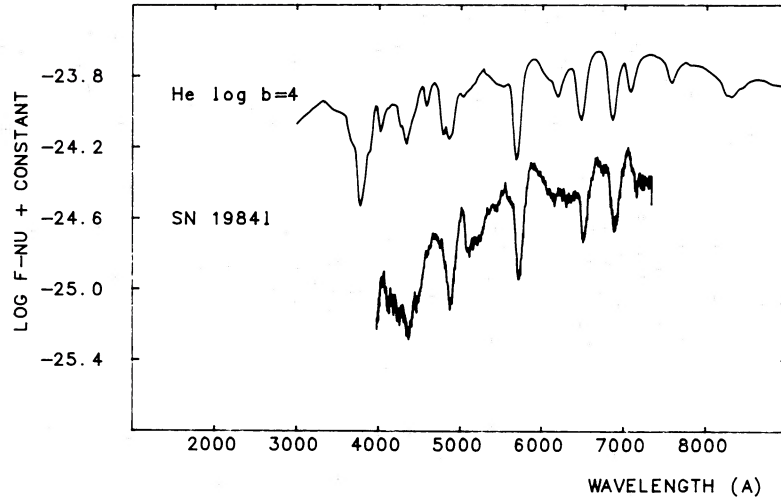


FIG. 8.—The spectrum of SN 1984L about 20 days after maximum (September 23) is shown in comparison with the theoretical calculation of Fig. 5 with $b = 10^4$. No change in temperature or density is invoked in the model to allow for the expansion subsequent to maximum light, but the relative strength and placement of the features, particularly of the strong He I lines at 4471, 5876, 6678, and 7065 Å, are again in generally good agreement with the observed spectrum.

from nuclear statistical equilibrium, the $\sim 0.4 M_{\odot}$ of detonated He consists of 90% ^{56}Ni and 5% He (Woosley, Taam, and Weaver 1986). In this model, the C/O core expands unburned, the potential origin of the oxygen enrichment in the supernebular phase. Branch and Nomoto show that for an appropriate choice of the optical depths of Fe II and He I a synthetic spectrum can reproduce the observed spectrum of SN 1984L (August 30). This calculation does not, however, specifically constrain the abundances of Fe and He. The current models are more nearly physically self-consistent in that while a departure coefficient is assumed for He, the effect of Fe is computed rigorously for the assumed structure under the assumption of LTE. Figures 7 and 8 show that the blue end of the spectrum is adequately represented by Fe in only solar proportions. To check the effect of enhanced Fe abundance, a model was calculated with a density profile of $\rho \propto r^{-7}$, $b = 10^4$ for He, and mass fractions $X_{\text{He}} = 0.64$, $X_{\text{O}} = 0.26$, $X_{\text{Fe}} = 0.1$ giving a ratio

for Fe/He which is enhanced considerably over the previous calculations but still much less than that demanded by the model of Branch and Nomoto. The result is shown in Figure 9. At even 10% by mass the Fe II lines are far too strong not only in the blue, but throughout the optical portion of the spectrum. Note from Table 3 that with the relatively compact atmosphere associated with the $\rho \propto r^{-7}$ density profile the temperature is everywhere in excess of 5000 K. Singly ionized iron would not exist if it were not for the rather large density compared, for instance, to a deflagration model for a SN Ia at a time of about 15 days after the explosion. As a further check on the model dependence of our conclusion that SN Ib are not highly iron-enriched, a spectrum was also calculated for a model consisting of the incineration of a degenerate helium white dwarf of $\sim 0.6 M_{\odot}$. This model is more in the direct spirit of the suggestion of Branch and Nomoto, although it does not contain the lagging C/O core. The composition was

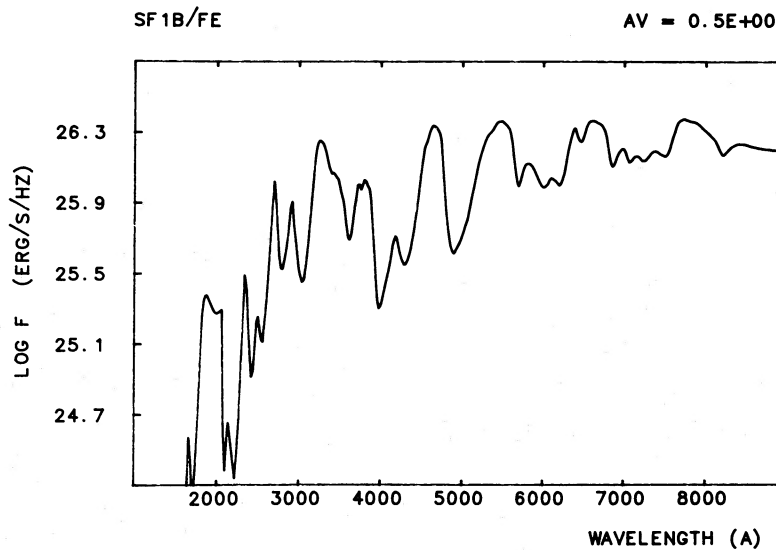


FIG. 9.—A theoretical spectrum is presented for the model of Figs. 5 and 6, with departure coefficient $b = 10^4$, but with a composition of approximately $X_{\text{He}} = 0.64$, $X_{\text{O}} = 0.26$, $X_{\text{Fe}} = 0.10$, i.e., a strongly enhanced iron abundance. Despite the large departure coefficient for helium, the spectrum is dominated by excessively strong lines of Fe II and bears little relation to the observed spectra of Type Ib supernovae.

taken to be an appropriate mix of Ni, Co, and Fe, corresponding to the epoch of maximum light. The expected small helium abundance after freezeout was omitted. The spectrum (not shown) failed to resemble either a SN Ia or Ib in any significant way. These two atmosphere calculations seem to be substantial evidence that models based on detonations in white dwarfs, which demand a large abundance of Fe and a large Fe/He ratio, are not viable models for the origin of SN Ib. Only if non-LTE effects alter the iron spectrum in a major way could such models correspond to the observed spectra.

V. DISCUSSION AND CONCLUSION

The evidence for extreme Population I environments, circumstellar nebulae, and estimates of the ejecta mass based on emission-line strengths in the supernebular phase all suggest that SN Ib have their origin in the hydrogen-denuded cores of massive stars. The results presented in this paper represent a crucial, if still qualitative, enhancement of this point of view.

The atmosphere calculations confirm beyond any reasonable doubt that He exists in substantial amounts in the portions of the ejecta that are observable up to 2 months after maximum light in SN 1983N and SN 1984L. An important prediction that follows from this conclusion is that the 10380 Å line of He I should be a very strong infrared feature if the level populations are at all similar to those assumed here. The helium abundance probably cannot be as low as 0.1 by mass without requiring an implausibly large departure from LTE. The other principal constituent is probably oxygen, given the large oxygen abundance observed at late times and the need for a plentiful supply of free electrons beyond those available from helium alone. Spectra of SN Ib extending to 8000 Å are needed to determine the existence of the oxygen in the early phases. Carbon is also identified in the early and late phases and probably contributes substantially to the mass fraction of the ejecta. Iron features are seen, but the iron abundance of the matter seen near maximum light need not exceed the solar ratio. The composition used to reproduce the observed spectra, predominantly helium and oxygen, with a solar mix of heavier elements is representative of the composition of models of massive stars and hence more evidence that SN Ib have their origin in the cores of massive stars.

The phrase "born old" used to describe the resemblance of maximum light SN Ib to postmaximum SN Ia suggests a physical relation between the two classes of supernovae. Figure 3 and the current models show that the similarity is restricted, qualitative, and fleeting. The spectra of SN Ia and Ib are very different for $\lambda > 6000$ Å. The absorption minimum at ~ 5800 Å in the March 27 spectrum of SN 1981B has a qualitative similarity to the 5700 Å minimum in SN 1983N and 1984L, but we now see that the latter is probably primarily due to He I $\lambda 5876$ and the former to Fe II or perhaps Na I (Branch *et al.* 1983), so the resemblance is mostly a coincidence. There are peaks in the maximum light SN Ib spectra and the postmaximum SN Ia spectrum at 4500 Å, but the peak is much narrower in the SN Ia. The spectra of SN Ia in this wavelength range evolve only slowly, while those of SN Ib show significant quantitative changes as the helium lines become sharper and deeper with age. While the blue spectra of SN Ia are probably due essentially entirely to Fe II, even the qualitatively similar features in the SN Ib are shaped by the added presence of He, Mg, and other species. The phrase "born old," while catchy, thus seems to have very limited physical significance and does not necessarily imply common progenitors or explosion mechanisms for SN Ia and Ib.

Branch and Venkatakrishna (1986) have modeled the portion of the spectrum of the SN Ia 1981B between 2800 and 3400 Å with blends of Fe II and Co II lines with $v \sim 12,000$ km s^{-1} , consistent with the expected composition of an exploding white dwarf. They argue that the premaximum ultraviolet spectrum ($\lambda \leq 3100$) of the SN Ib 1983N is very similar to that of SN 1981B (Panagia 1985) and hence that the composition and the underlying cause of the explosion are likely to be closely related. They point out that a Wolf-Rayet star would not be expected to eject iron and cobalt at high velocities. This motivation leads Branch and Nomoto (1986) to present their model for the explosion of SN Ib based on the detonation of a layer of degenerate helium surrounding a degenerate C/O core. An immediate problem with this model is that, unlike observed SN Ib, the light curve of this detonation model evolves more rapidly than models of SN Ia assuming the same opacity ($\kappa \sim 0.1$ cm² g⁻¹; Woosley, Taam, and Weaver [1986]). The iron peak matter that dominates the outer ejecta in this model tends to have a lower opacity than the outer partially burned layers of the carbon deflagration models invoked for SN Ia (Harkness 1986), which would make the light curve evolution even quicker. This model is also difficult to reconcile with the association with H II regions which typify SN Ib.

The current calculations add another argument against an exploding white dwarf model for SN Ib. It is correct that a massive star model is not expected to show high-velocity cobalt prior to maximum light. The combined optical and ultraviolet spectra for SN 1983N (Panagia *et al.* 1987) do not, however, show strong evidence for the absorption dip at 3200 Å (primarily due to lack of relevant data) that seems to occur in SN 1981B and which is attributed to Co II (Branch *et al.* 1983). The models presented here show that the blue portion of the spectrum near maximum light can be reproduced by Fe II in both SN Ia and SN Ib, but with a large abundance of iron for SN Ia (~ 0.03 by mass) and a small abundance (~ 0.0018) for SN Ib. This difference in iron abundance for models of SN Ia and SN Ib shows that the spectra can be similar even though the underlying physical models are quite different. A more complete discussion of the optical and ultraviolet spectra of SN Ia and SN Ib is given by Harkness and Wheeler (1987). The current models for SN Ib argue that the iron mass fraction cannot be as large as 0.1 in SN Ib, a statement consistent with a massive star model in which the deep inner layers where Fe and Co may reside have not yet been exposed, and inconsistent with the off-center detonation model of Branch and Nomoto (1987).

Sramek, Panagia, and Weiler (1984) and Chevalier (1984) discuss the implications of the radio observations of SN 1983N for the progenitor. They note that the optical light curve precludes an explosion within a supergiant envelope and propose a symbiotic-type binary system with the supernova occurring in a white dwarf which is in turn immersed in the circumstellar nebula shed by an asymptotic giant branch companion. The objections to a white dwarf progenitor for SN Ib outlined above apply to this version as well. Furthermore, the lack of evidence for hydrogen in either the early or later supernebular phases may constrain this picture. The models for radio emission determine that $\dot{M}/v_w \sim 3 \times 10^{-7} M_\odot \text{ yr}^{-1} \text{ km s}^{-1}$ where \dot{M} is the mass-loss rate and v_w the wind velocity. The symbiotic star model is based on the assumption that $v_w \sim 10$ km s^{-1} and hence $\dot{M} \sim 3 \times 10^{-6} M_\odot \text{ yr}^{-1}$, consistent with a red supergiant. Alternatively, the radio emission might be explained with $\dot{M} \sim 3 \times 10^{-4} M_\odot \text{ yr}^{-1}$ and $v_w \sim 10^4$ km s^{-1} as expected for a Wolf-Rayet star. Chevalier assumed a

$\rho \propto r^{-7}$ profile patterned after an exploding white dwarf. The present spectral calculations give some independent justification for such a choice. This does not necessarily imply a white dwarf progenitor, however. The $n = 3$ polytrope structure shared by a white dwarf and a radiation-pressure dominated core might be expected to give rise to similar density profiles in the ejecta.

If one accepts a massive star origin for SN Ib, then there are many interesting questions concerning their origin which may be posed. Stars of different mass subjected to mass loss in a wind or to a binary companion will display different compositions at the time of explosion. Stars which are sufficiently massive ($\gtrsim 30 M_{\odot}$) to eject their hydrogen envelope in a wind and spontaneously become Wolf-Rayet stars are apt to have ejected their helium layers in the wind as well as before the explosion (Prantzos *et al.* 1986). The deduced large helium abundances in SN 1983N and SN 1984L thus argue that the progenitors of these SN Ib are less massive than this.

This conclusion is in keeping with the restrictions on the ejecta mass from the width of the peak of the light curve of SN 1983N (Wheeler and Levreault 1985) and with the requirement that the kinetic energy of the ejecta not be excessive, both of which suggest that the ejecta should not be more than several solar masses. A related factor concerns the rates of occurrence of SN Ib. Branch (1986) has argued that SN Ib, being fainter than SN Ia, are subject to a negative selection effect, and that SN Ib could occur at a rate comparable to SN Ia. In the last few years SN Ib have been discovered at a rate comparable to SN II, to which they are comparably bright. Hence, SN Ib may occur as often as SN II and derive from the same progenitor mass range, $\lesssim 20 M_{\odot}$.

An exciting challenge is to find an evolutionary origin for SN Ib in massive stars which is commensurate with the observational constraints on the light curve and spectra. Hot hydrogen-deficient stars have suggestive properties, although it is not clear that there are sufficient of them in the Galaxy to account for the expected rate (Uomoto 1986). Work is underway to calculate light curves for a range of realistic massive star models to determine more precise constraints on the mass of the ejecta (Sutherland, Cappellaro, and Wheeler 1987). Deeper understanding of the observed spectra will be obtained by first exploring a more extensive set of parameterized models. An important step will be to remove the restriction that the departure coefficient be constant in radius. Further in the future, an array of massive star models will be explored with atmosphere calculations to determine more precisely the sort of structure that will produce a theoretical spectrum in agreement with observations, not just at a single epoch, but as a function of time. Such calculations will constrain not only the mass of the core, but the degree of mass loss the progenitor star must have undergone prior to explosion. Analysis of the supernebulular phase will give an independent set of constraints on the structure, composition, and kinematics.

Care must be taken in future calculations to let the observed spectra and light curves be the guide. The actual structure of

SN Ib may not fit preconceived notions deriving either from observations or theory. Although it is tempting to associate SN Ib with Wolf-Rayet star progenitors, Wolf-Rayet stars as an observed class may prove too massive ($\gtrsim 10 M_{\odot}$) to satisfy the observational constraints of the SN Ib. Evolutionary calculations of Wolf-Rayet models with mass loss have not yet proceeded to the epoch of core collapse, and it is possible that a late, very heavy mass-loss phase will reduce even a $10 M_{\odot}$ Wolf-Rayet star to $3-4 M_{\odot}$ at the time of explosion, but this can only occur at the expense of drastically reducing the helium abundance in violation of the conditions determined here. Likewise, evolutionary calculations will give more self-consistent initial models, but given uncertainties associated with assumptions of spherical symmetry, and a general lack of knowledge of the effects of time-dependent convection on the very late stages of stellar evolution, it will not be surprising if current theory does not give a precise fit to observations.

On the contrary, SN Ib represent an immensely valuable new laboratory to study the late stages of massive star evolution by providing a source of direct observational constraints to guide theoretical studies. Prior to the elucidation of the nature of SN Ib the great deal of work on massive star core evolution and collapse has proceeded in the absence of all but the most basic observational checks: Does a model explode or not, and, if so, with what kinetic energy? Nucleosynthesis gives an indirect constraint subject to the uncertainties of the mass function and Galactic evolution. Type II supernovae are thought to be produced, in some instances at least, by core collapse, but the physically interesting regions are shielded from view by the enshrouding hydrogen envelope and only the most basic kinematic constraints have emerged. SN Ib in the early atmosphere and late supernebulular phases now give a way to determine the density, temperature, and composition structure of the cores of massive stars. This in turn will surely lead to important new insights into the physical processes in the star prior to and during the explosion and ultimately, perhaps, to an understanding of the explosion mechanism itself.

We thank Allen Shafter, David Branch, Ken Nomoto, Zalman Barkat, James Graham, and Peter Conti for valuable conversations. The research of R. P. H. and J. C. W. is supported in part by NSF grant 8413301 and by a grant of computer time from Cray Research, Inc. J. C. W. is grateful for the hospitality of the Aspen Center for Physics where portions of this manuscript were written. R. A. D. is supported by NASA contract NAS 5-24463 and thanks Ann Wehrle for obtaining the Mount Lemmon data. The Mount Lemmon image-tube scanner is supported by NSF grant AST 78-09228 to UCSD. A. U. is supported by STScI grant CW00485 and thanks Dennis Hegyi for the use of his CCD camera and Donald Gudehus for assistance at the telescope. The observations of E. S. B. and A. L. C. are supported by NASA grant NGR 44-012-152. H. L. D. and D. R. G. are supported by NSF grant AST 8314962 and Welch Foundation grant F-910.

REFERENCES

- Allen, C. W. 1973, *Astrophysical Quantities* (3d ed.; London: Athlone Press).
 Bertola, F. 1964, *Ann. d'Ap.*, **27**, 319.
 Branch, D. 1986, *Ap. J. (Letters)*, **300**, L51.
 Branch, D., Doggett, J. B., Uomoto, K., and Thielemann, F. K. 1985, *Ap. J.*, **294**, 619.
 Branch, D., Lacy, C. H., McCall, M. L., Sutherland, P. G., Uomoto, A., Wheeler, J. C., and Wills, B. J. 1983, *Ap. J.*, **270**, 123.
 Branch, D., and Nomoto, K. 1986, *Astr. Ap.*, **164**, L13.
 Branch, D., and Venkatakrisna, K. L. 1986, *Ap. J. (Letters)*, **306**, L21.
 Buta, R. 1984, *IAU Circ. No.* 3981.
 Chevalier, R. A. 1984, *Ap. J. (Letters)*, **285**, L63.
 Elias, J. H., Matthews, K., Neugebauer, G., and Persson, S. E. 1985, *Ap. J.*, **296**, 379.
 Filippenko, A. V. and Sargent, W. L. W. 1985, *Nature*, **316**, 407.

- Filippenko, A. V. and Sargent, W. L. W. 1986, *A.J.*, **91**, 691.
 Gaskell, C. M., Cappellaro, E., Dinerstein, H., Garnett, D., Harkness, R. P., and Wheeler, J. C. 1986, *Ap. J. (Letters)*, **306**, L77.
 Graham, J. R., Meikle, W. P. S., Allan, D. A., Longmore, A. J., and Williams, P. M. 1986, *M.N.R.A.S.*, **218**, 93.
 Harkness, R. P. 1985, in *Supernovae as Distance Indicators*, ed. N. Bartel (Berlin: Springer-Verlag), p. 183.
 ———, 1986, in *Radiation Hydrodynamics in Stars and Compact Objects*, ed. D. Mihalas and K.-H. A. Winkler (Berlin: Springer-Verlag), p. 166.
 ———, 1987, in preparation.
 Harkness, R. P., and Wheeler, J. C. 1987, in preparation.
 Höflich, P., Wehrse, R., and Shaviv, G. 1986, *Astr. Ap.*, **163**, 105.
 Kirshner, R. P. 1986, private communication.
 Panagia, N. 1985, *Supernovae as Distance Indicators, Lecture Notes in Physics*, ed. N. Bartel, **224**, 14.
 Panagia, N., *et al.* 1987, in preparation.
- Panagia, N., Sramek, R. A., and Weiler, K. W. 1986, *Ap. J. (Letters)*, **300**, L55.
 Prantzos, N., Doom, C., Arnould, M., and de Loore, C. 1986, *Ap. J.*, **304**, 695.
 Pskovskii, Y. P. 1970, *Soviet Astr.*, **14**, 798.
 Richter, O.-G., and Rosa, M. 1984, *Astr. Ap.*, **140**, L1.
 Sramek, R. A., Panagia, N., and Weiler, K. W. 1984, *Ap. J. (Letters)*, **285**, L63.
 Sutherland, P. G., Cappellaro, E., and Wheeler, J. C. 1987, in preparation.
 Uomoto, A. 1986, preprint.
 Uomoto, A., and Kirshner, R. P. 1985, *Astr. Ap.*, **149**, L7.
 Wheeler, J. C., and Harkness, R. P. 1986, *Proc. NATO Advanced Study Workshop on Distances of Galaxies and Deviation from the Hubble Flow*, ed. B. Madore and R. B. Tully (Dordrecht: Reidel), p. 45.
 Wheeler, J. C., Harkness, R. P., Barkat, Z., and Swartz, D. 1986, *Pub. A.S.P.*, **98**, 1018.
 Wheeler, J. C., and Levreault, R. 1985, *Ap. J. (Letters)*, **294**, L17.
 Woosley, S. E., Taam, R. E. and Weaver, T. A. 1986, *Ap. J.*, **301**, 601.

E. S. BARKER, A. L. COCHRAN, H. L. DINERSTEIN, D. R. GARNETT, R. P. HARKNESS, and J. C. WHEELER: Department of Astronomy, University of Texas, Austin, TX 78712

R. A. DOWNES: Applied Research Corporation, 8201 Corporate Drive, Suite 920, Landover, MD 20785

R. P. KIRSHNER and R. LEVREULT: Harvard University, Center for Astrophysics, 60 Garden Street, Cambridge, MA 02138

B. MARGON: Department of Astronomy, University of Washington, Seattle, WA 98195

A. UOMOTO: The Johns Hopkins University, Homewood Campus, Baltimore, MD 21218